Investigation of the Transient Characteristics of a Micro Heat Pipe

D. Wu* and G. P. Peterson†
Texas A&M University, College Station, Texas 77843

An analytical investigation was conducted to determine the potential advantages of incorporating very small (100 μm) "micro" heat pipes directly into semiconductor devices. As a result of this investigation, a transient numerical model capable of predicting the thermal behavior of these micro heat pipes during startup or variation in the evaporator thermal load was developed. This numerical model was used to identify, evaluate, and better understand the phenomena that govern the transient behavior of micro heat pipes as a function of the physical shape, the properties of the working fluid, and the principal dimensions. The modeling results were compared with the steady-state results from an earlier experimental investigation and were shown to accurately predict the steady state dry out limit for two different test pipes. Using the verified numerical model, the parameters that affect the axial heat transport capacity were evaluated. The results of this evaluation indicate that in micro heat pipes reverse liquid flow occurs in the liquid arteries during startup and/or rapid transients. In addition, the wetting angle was found to be one of the most important factors contributing to the transport capacity.

Nomenclature

A = cross-sectional area
C_p = specific heat
d = distance
j = evaporation
M = molecular weight
$\dot{m}$ = mass flow rate
P = pressure
Q = heat transfer
$\dot{q}$ = heat transfer rate
R = universal gas constant
r = radius of curvature
T = temperature
t = time
V = velocity
W = wetted perimeter
x = length or distance
y = distance
β = dimensionless parameter (see Fig. 2)
θ = wetting angle
λ = latent heat
μ = viscosity
ρ = density
σ = surface tension

Subscripts

a = adiabatic
b = boundary
c = capillary, curvature
d = diagonal
e = evaporator
ec = evaporation-condensation
f = friction
h = hydraulic
l = liquid
m = momentum, mean
o = outer
p = pipe
s = solid
v = vapor, viscous

Received Sept. 25, 1989; presented as Paper 90-0060 at the AIAA 28th Aerospace Sciences Meeting, Reno, NV, Jan. 8–11, 1990; revision received Mar. 12, 1990.

*Research Associate, Department of Mechanical Engineering. Member AIAA.
†Associate Professor of Mechanical Engineering. Member AIAA.

Introduction

BECAUSE of the high heat fluxes associated with power transistors, LSI and VLSI circuits, and avionics packages, it is necessary to develop new methods for removing heat from modern electronic devices. A recent review of thermal control techniques in electronic components and devices[1] included a proposal for using very small heat pipes embedded in individual silicon or gallium arsenide chips to eliminate localized hot spots. This concept, which was first introduced by Cotter,[2] involves the use of small heat pipes of triangular cross section, approximately 100 μm on a side, to distribute the heat more uniformly throughout the semiconductor devices and thereby lower the junction temperatures and improve the device reliability. Several alternative applications exist, including providing active cooling to the condenser portion of these heat pipes to allow heat generated within the chip to be completely removed. Because these heat pipes would typically be on the order of 100–200 μm, they are referred to as "micro" heat pipes. Although the original concept proposed by Cotter[2] involved the use of anisotropic etchants to form the heat pipe channels, alternative construction techniques have been developed[3] and several test pipes with diameters on the order of 100 μm have been constructed and tested.

In the original presentation of Cotter, a micro heat pipe was defined as "a heat pipe so small that the mean curvature of the vapor-liquid interface is necessarily comparable in magnitude to the reciproeal of the hydraulic radius of the total flow channel." This definition was later refined by Babin et al.[4] and expressed mathematically to define a micro heat pipe as one that satisfies the condition

$$r_c/r_h \geq 1 \tag{1}$$

where r_c is the capillary radius of the heat pipe and r_h is the hydraulic radius of the flow channel. In practical terms, a micro heat pipe is a wickless, noncircular channel with an approximate diameter of 100–1000 μm and a length of about 10–100 mm.

Babin et al.[4] investigated the steady-state behavior of several micro heat pipes with outer dimensions of 1 × 1 mm and

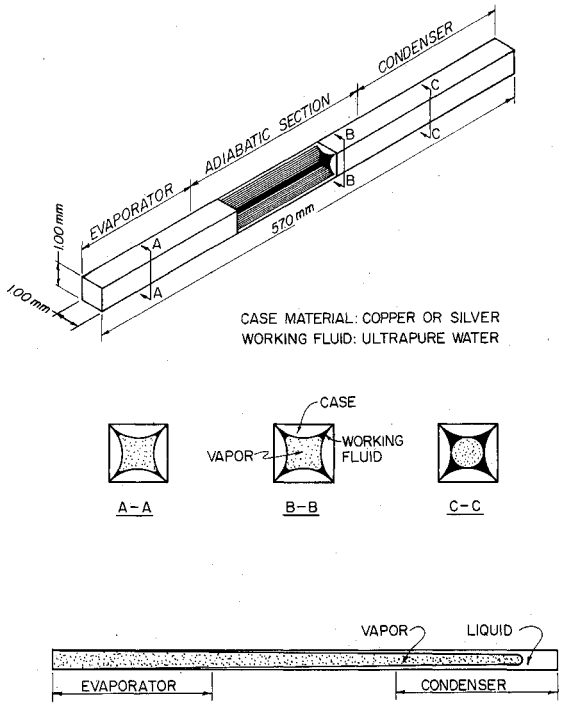

Fig. 1 Trapezoidal micro heat pipe.

lengths of approximately 57 mm. As illustrated in Fig. 1, the internal shape of these devices is a concave trapezoid with tapered triangular channels in each of the four corners. Because of the small radius of curvature within these channels, the corner regions serve as liquid arteries, producing high capillary pressure that promote flow of the liquid from the condenser to the evaporator. Using the conventional total pressure drop method outlined by Chi[5] and Dunn and Reay,[6] Babin et al. developed an analytical model capable of predicting the steady-state transport limitations. The results of this model, which were verified experimentally, indicated that during steady-state operation, the capillary limit was the predominant one and occurred well below the viscous, boiling, entrainment, and sonic limits.

Although the heat pipes investigated by Babin et al. are not small enough to be fabricated as an integral part of semiconductor devices, the fundamental behavior is similar to that occurring in the smaller versions, ones with cross-sectional dimensions of 100–200 μm and smaller, provided that these dimensions do not restrict free molecular flow. To better understand the effects of variations in the geometry, the liquid-solid wetting angle, the amount of working fluid, and continued size reductions, a transient model capable of predicting the behavior of these heat pipes during startup or variations in the thermal load was developed.

Analytical Model

The high thermal conductivity of heat pipes is the result of the evaporation and condensation process occurring within the heat pipe. For this reason, determination of the evaporation and condensation rate of the liquid plays a key role in evaluating the thermal characteristics and heat transport limitations of these heat pipes. In the present model, an expression for the free molecular flow mass flux of evaporation j, presented by Collier[7] and later used by Colwell and Chang,[8] was employed. This relationship is

$$j = \left[\frac{M}{(2\pi RT)}\right]^{0.5}(P_s - P_v) \tag{2}$$

When P_s is greater than P_v, j is positive and the liquid evaporates. When P_s is less than P_v, j is negative and the vapor condenses. In the development of the numerical model presented here, the evaporation-condensation rate was assumed to be proportional to the liquid-vapor interface area in each section of the heat pipe, i.e.,

$$\Delta\dot{m}_{ec} = j\,\Delta A_{ec} = jW_{ec}\Delta x \tag{3}$$

where ΔA_{ec} is the evaporation-condensation surface area in one section, W_{ec} the perimeter of the liquid-vapor interface, and Δx the section length.

For a given latent heat λ, the rate of the heat released or absorbed in any section can be determined from

$$\Delta Q_{ec} = \lambda\,\Delta\dot{m}_{ec} \tag{4}$$

For a heat pipe to operate properly, the capillary pressure must be sufficient to overcome the difference of the liquid and vapor pressures, or

$$P_{vl} = P_v - P_l = \sigma/r_c \tag{5}$$

where r_c is the radius of curvature of the liquid-vapor interface. Since both P_{vl} and r_c are functions of the axial position, the derivative of the above equation yields

$$\frac{dP_{vl}}{dx} = \frac{-\sigma}{r_c^2}\frac{dr_c}{dx} \tag{6}$$

Expressing this over a finite interval yields

$$\Delta P_{vl} = (-\sigma/r_c^2)\Delta r_c \tag{7}$$

where

$$\Delta P_{vl} = \Delta P_{fv} + \Delta P_{mv} + \Delta P_{fl} + \Delta P_{ml} \tag{8}$$

The pressure changes are those due to the liquid and vapor friction and the momentum changes are those occurring in any one section along the heat pipe.

Based on the momentum equation, the pressure drops due to friction for laminar flow can be expressed as

$$\Delta P_f = (2\mu\,\Delta xV)/r_h^2 \tag{9}$$

where r_h is the hydraulic radius, and V is the velocity of the flow that is equal to a function of the mass flow rate, the density, and the area.

The total pressure drop due to the momentum change can be expressed as

$$\Delta P_m = (V\,\Delta\dot{m} + \dot{m}\,\Delta V + \Delta\dot{m}\,\Delta V)/A \tag{10}$$

The energy equation used in this model can be written as

$$Q_{in} = Q_{out} + Q_r \tag{11}$$

$$Q_r = \int \rho_l A_l C_{Pl}\,\Delta T_l\,dx + \int \rho_v A_v C_{Pv}\,\Delta T_v\,dx + \int \rho_s A_s C_{Ps}\,\Delta T_s\,dx \tag{12}$$

C_{Pl}, C_{Pv}, and C_{Ps} are the heat capacities of the liquid, vapor, and solid boundaries, respectively, and ΔT is the corresponding temperature change.

The continuity equation can be written as

$$\int \rho_v A_v\,dx + \int \rho_l A_l\,dx = \text{const} = \text{fluid charge} \tag{13}$$

and the total volume inside the heat pipe can be defined and expressed, respectively, as

$$\text{vol} = \text{vol}_l + \text{vol}_v \tag{14a}$$

$$A = A_l + A_v \tag{14b}$$

As is the case for larger heat pipes, micro heat pipes consist of three basic sections, an evaporator and a condenser, separated by an adiabatic section. Each section has a different set of boundary conditions and as a result has been treated independently.

Evaporator Region

The single boundary condition used in the evaporator section is the time dependent heat flux. For a specific input heat flux, the saturation pressure at a given location can be obtained by using a combination of the mass flux expression given in Eq. (2) and the energy conservation equation given in Eq. (12). Assuming that a temperature change at the boundary yields a corresponding temperature change of the liquid, and neglecting the temperature gradient in the liquid (the liquid-vapor interface is only a small percentage of the total interface area), these equations take the following form:

$$P_s = \frac{\dot{q}_{ec}}{(M/2\pi RT_l)^{1/2}\,\Delta x W_{ec}\lambda} + P_v \tag{15}$$

$$\dot{q}_l = (C_{Pl}\rho_l A_l\,\Delta x\,\Delta T_l)/\Delta t \tag{16}$$

$$\dot{q}_s = (C_{Ps}\rho_s A_s\,\Delta x\,\Delta T_s)/\Delta t \tag{17}$$

$$\dot{q}_{in} = \dot{q}_{ec} + \dot{q}_l + \dot{q}_s \tag{18}$$

Since T_l is a function of P_s, Eqs. (15–18) are coupled and can be solved using an iterative method with relaxation to obtain values for T_l, $\dot{q}_{ec}$, $\dot{q}_l$, and $\dot{q}_s$. Because the difference between the boundary and liquid temperatures ΔT_{bl} is proportional to the input heat flux, the boundary temperature can be obtained by adding ΔT_{bl} to T_l.

Adiabatic Region

In the adiabatic section, the latent heat absorbed by evaporation and given up by condensation is equal to the sensible heat absorbed or rejected by the liquid and/or the heat pipe case. The governing equations for each element in this section can therefore be expressed as

$$\dot{q}_{ec} = \lambda W_{ec}\,\Delta x[M/(2\pi RT_l)]^{1/2}(P_s - P_v) \tag{19}$$

$$\dot{q}_1 = (C_{Pl}\rho_l A_l\,\Delta T_l\,\Delta x)/\Delta t \tag{20}$$

$$\dot{q}_s = (C_{Ps}\rho_s A_s\,\Delta T_b\,\Delta x)/\Delta t \tag{21}$$

$$\dot{q}_{ec} + \dot{q}_l + \dot{q}_s = 0 \tag{22}$$

By assuming no temperature drop at the liquid/case boundary, i.e., $T_l = T_b$, Eqs. (19–22) can also be solved using an iterative technique to obtain q_{ec}, $\dot{q}_l$, $\dot{q}_s$, and ΔT_l.

Condenser Region

In the condenser region, the boundary temperature of the heat pipe was assumed to be constant, resulting in governing equations similar to those used in the adiabatic section,

$$\dot{q}_{ec} = \lambda W_{ec}\,\Delta x[M/(2\pi RT_l)]^{1/2}(P_s - P_v) \tag{23}$$

$$\dot{q}_l = (C_{Pl}\rho_l A_l\,\Delta T_l\,\Delta x)/\Delta t \tag{24}$$

$$\dot{q}_s = \frac{C_{Ps}\rho_s A_s\,\Delta T_b\,\Delta x}{\Delta t} \tag{25}$$

$$\dot{q}_{ec} + \dot{q}_l + \dot{q}_s = \dot{q}_{out} \tag{26}$$

Although in normal operation the condenser boundary temperature would vary with the input power, in a controlled laboratory experiment this condition is easily obtained by controlling the temperature and/or flow rate of the condenser coolant.

General Assembly

Because the evaporation-condensation rate is extremely sensitive to changes in the vapor pressure, a predictor-corrector treatment was applied to obtain a stable solution. Initially, the evaporation rate was assumed to be equal to the condensation rate, and the vapor pressure was calculated. This vapor pressure was then used to compute the change in the mass of vapor and, hence, the difference between evaporation and condensation. The original assumption of equal evaporation and condensation rates was then checked and the values updated. Preliminary tests indicated that the solution was stable regardless of the time step size used. In comparison, prior to using this predictor-corrector treatment, the solution vibrated with increasing magnitude for time step sizes below 0.01 ms.

The solution procedure consisted of initializing the variables and arrays and by iteration, computing the boundary, liquid, and vapor temperatures along with the evaporation and condensation rates, the pressure drops, and the flow rates for each section. The resulting radii of curvature for the liquid-vapor interface was then computed and the liquid-vapor mass flow rate corrected using the resulting vapor pressure.

Because both the steady state and transient performance of the heat pipe are strongly dependent upon the physical geometry, it was necessary to accurately describe the geometry mathematically. For the heat pipes considered in this investigation, the liquid cross-sectional area of a single channel was defined in terms of the geometry, shown in Fig. 2, as

$$A_l = xy - r_s^2(\gamma - \sin\gamma) - (r^2/2)(\beta - \sin\beta) \tag{27}$$

Once this had been done, it was necessary to determine the wetting angle θ where

$$\theta = \cos^{-1}[(\sigma_{sv} - \sigma_{sl})/\sigma_{lv}] \tag{28}$$

Although some information was available in the literature on the surface tension between the case, copper or silver, and the

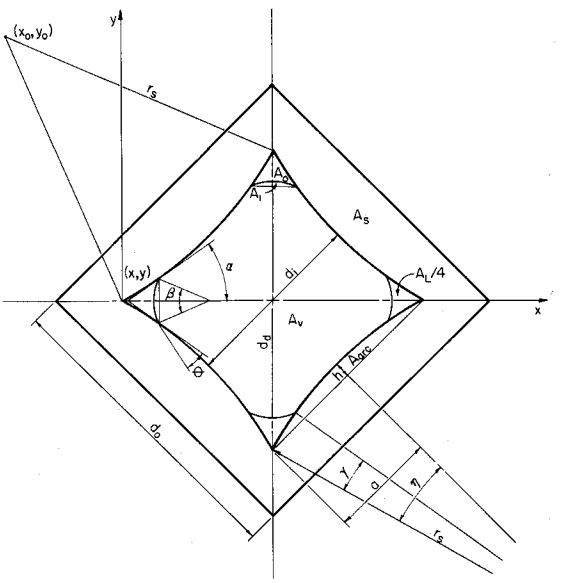

Fig. 2 Cross-sectional shape of the modeled heat pipe.

working fluid, water, only limited information on the surface tension between the solid and the vapor σ_{sv} and the liquid and the vapor σ_{lv} was available. For this reason, an experimental investigation was conducted to determine the wetting angle.

Determination of the Wetting Angle

An acrylic chamber with internal dimensions of approximately $2.54 \times 2.54 \times 8$ cm was constructed. The front and back walls of the chamber were transparent, whereas the left and right sides were made of copper and silver, respectively. The chamber was filled with approximately 10 cm^3 of distilled water through a fill port located in the top and evacuated for approximately 5 min to eliminate noncondensible gases. After filling, the fill port was closed and sealed. By tilting the chamber until the liquid at the interface formed a flat surface, the wetting angle could be measured. The results of these experimental tests indicated wetting angles of 55 and 45 deg for copper and silver, respectively. Although heat pipes are normally baked out in a hard vacuum prior to charging, which effectively removes most adsorbed species and results in a lower contact angle than normally obtained without the bake out procedure, the values given above compare favorably with those of other investigators.

Results and Discussion

To verify the numerical model, the physical dimensions of the heat pipe tested by Babin et al.,[4] an outer diameter of 1 mm, inner diameter of 0.6 mm, and a diagonal of 1.0 mm along with evaporator and condenser lengths of 12.7 mm each, were used as inputs to the numerical model. Comparisons of the experimentally determined maximum heat transfer capacity and the steady-state capillary limit as predicted by the transient numerical model were then made for two test pipes. One heat pipe was constructed of copper and the other of silver, and both used ultrapure water as the working fluid.

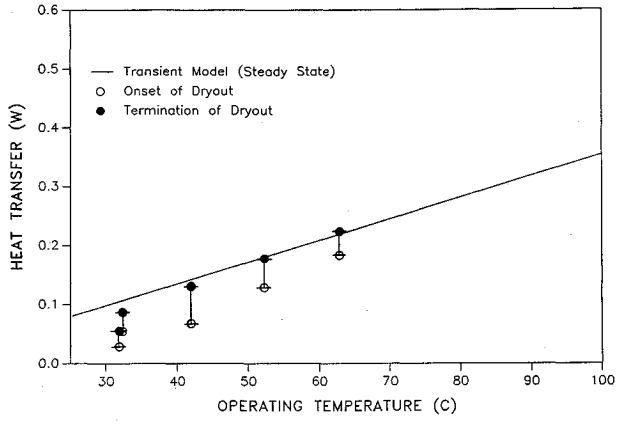

Fig. 3 Comparison of the maximum heat transport capacity of a trapezoidal micro heat pipe as a function of the operating temperature (silver, 0.0032 g charge).

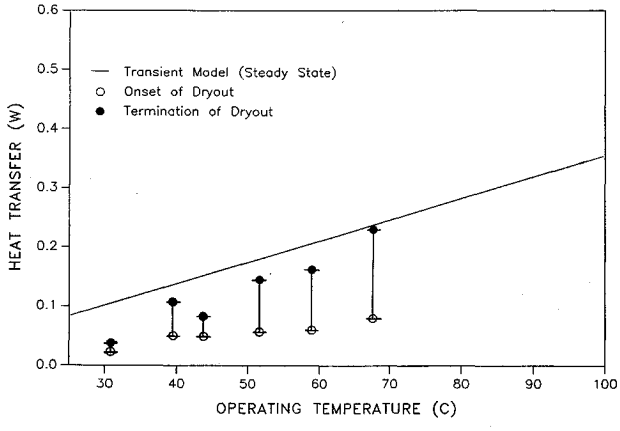

Fig. 4 Comparison of the maximum heat transport of a trapezoidal micro heat pipe as a function of the operating temperature (copper, 0.0032 g charge).

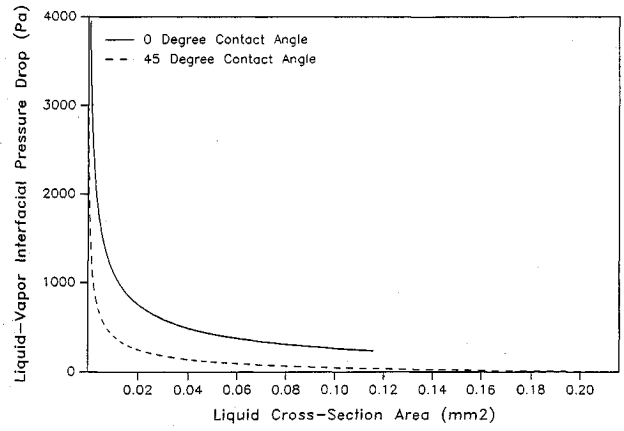

Fig. 5 Comparison of the interfacial pressure drop as a function of the liquid cross-sectional area.

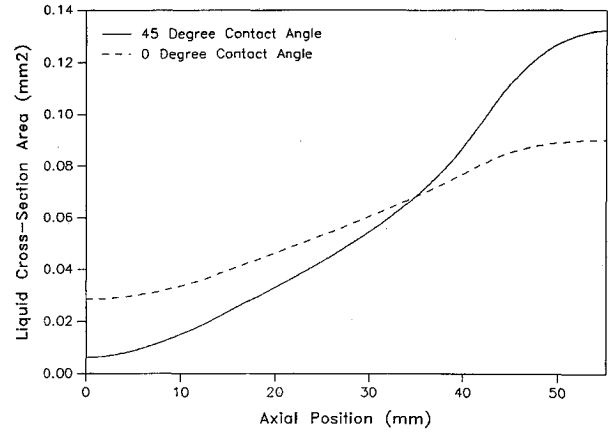

Fig. 6 Steady-state liquid cross-sectional area as predicted by the transient model.

Figures 3 and 4 illustrate the results of these comparisons. As shown, the transient model predicts the maximum steady-state heat transport capacity prior to the termination of dry out to within $\pm 5\%$ for the silver test pipe and $\pm 10\%$ for a majority of the experimental data obtained for the copper test pipe. It should be noted that, although the experimental tests were conducted in a vacuum, when the condenser temperature was greater than the ambient temperature, a small amount of power was required to maintain a uniform temperature along the pipe. Therefore, to determine the amount of heat transferred through the test pipe, shown on the ordinate in Figs. 3 and 4, this initial power was subtracted from the measured power input.

Once it had been demonstrated that the transient model could be used to accurately predict the steady-state heat-transfer limit, the model was used to determine the significance of the various parameters that govern the transient operation of micro heat pipes. Figure 5 compares the liquid cross-sectional area with the liquid-vapor interfacial pressure drop for wetting angles for both 0 and 45 deg. As illustrated, the maximum liquid cross-sectional area for a wetting angle of 45 deg is 0.218 mm^2, much larger than the 0.116 mm^2 for a wetting angle of 0 deg.

In Fig. 6, the difference between the minimum liquid area in the evaporator and the maximum liquid area in the condenser is shown to be significantly greater for the 45 deg wetting angle than for the case of the 0 deg wetting angle given the same axial heat flux. Also, near dry out, the frictional pres-

sure drop in the evaporator is much larger for the 45 deg wetting angle than for the 0 deg case as illustrated in Fig. 7. As a result, it is apparent that changes in the wetting angle cause large differences in the liquid pressure drop and hence the required capillary pumping pressure.

The relationships described above do not necessarily mean that large wetting angles will result in a larger maximum heat transport capacity, since the heat transport capacity is also dependent upon the liquid charge within the heat pipe. Using a fill charge of 0.32 mg and a 31°C condenser temperature, a maximum heat transport capacity of 0.11 W was predicted for a 45 deg wetting angle as compared to 0.12 W for a 0 deg wetting angle. Although the maximum heat transport capacity was similar, the limiting condition for the 45 deg wetting angle was dry out, whereas for the 0 deg wetting angle, the limiting condition resulted from condenser flooding.

In addition to affecting the pressure drops, the transient analysis indicated that the time required for the heat pipe to reach steady-state was longer for larger wetting angles. Once a heat input of 0.1 W had been reached, a total of 80 s was required for the heat pipe to reach steady state for wetting angles of 45 deg whereas only 30 s were required for a wetting angle of 0 deg. Because of the geometrical shape of the heat pipe, a phenomena referred to as an inverted meniscus was predicted to occur at wetting angles greater than 45 deg for liquid contact close to the midpoint of each side. This phenomena can best be described as a change in the shape of the liquid-vapor interface from one which is convex to one which is concave. From the above analysis, it is apparent that the wetting angle is one of the key parameters in the determination of the optimum charge and the heat transport capacity of the heat pipe.

The steady-state temperature profile, as predicted by the transient model, is illustrated in Fig. 8 for an input power of 0.1 W and a wetting angle of 45 deg. As shown, the liquid, vapor, and boundary temperatures are all the same at the left end of the pipe. This point represents the highest temperature within the pipe. From this maximum temperature, the vapor temperature decreases slightly in the evaporator region and then remains essentially constant throughout the adiabatic and condenser regions. The boundary and liquid temperatures decrease somewhat more rapidly in the evaporator region and continue to decrease in both the adiabatic and condenser regions. The two large gradients occurring at the exit to the evaporator and the entrance to the condenser are the result of longitudinal step size used in the model.

The transient numerical model indicates that the vapor temperature variations are proportional to the heat input and that without dry out or flooding, the conductivity of the heat pipe is independent of time. In contrast, a fairly long period of time is required for the other thermal hydraulic parameters to reach their steady-state values. The time required for the case to reach steady state ranges from 30 to 80 s after full heat input, depending on the wetting angle. The smaller the wetting angle and the higher the temperature, the shorter the time required.

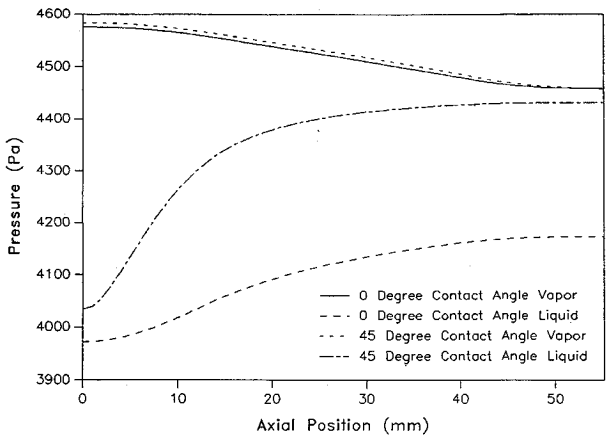

Fig. 7 Steady-state liquid and vapor pressure as a function of position as predicted by the transient model.

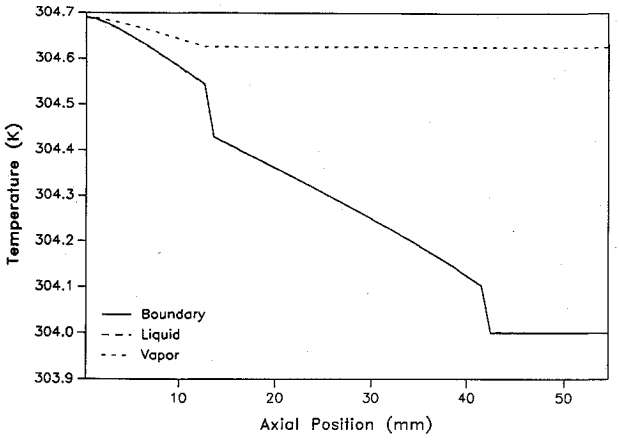

Fig. 8 Steady-state temperature distributions as predicted by the transient model.

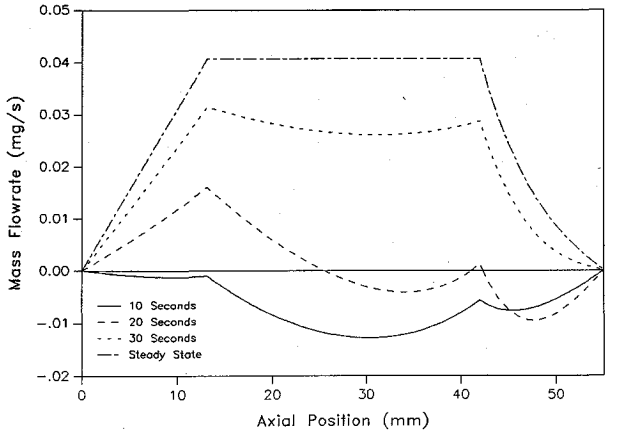

Fig. 9 Liquid mass flow rate as a function of time and the axial position.

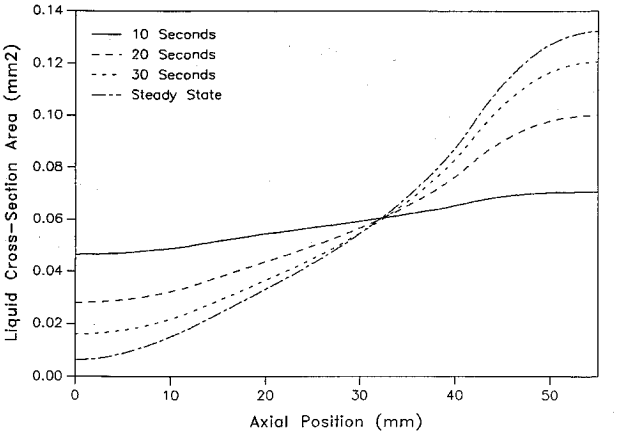

Fig. 10 Liquid cross-sectional area as a function of time and the axial position.

Figures 9 and 10 illustrate the changes in the liquid mass flow rate and liquid cross-sectional area as a function of time, respectively, for a power level of 0.1 W and a wetting angle of 45 deg. It is significant to note that during the time immediately after the application of the heat to the evaporator, the liquid and vapor flow in the evaporator are both in the same direction. This reverse liquid flow is the result of an imbalance in the total pressure drop. The evaporation rate does not provide an adequate change in the liquid-vapor interfacial

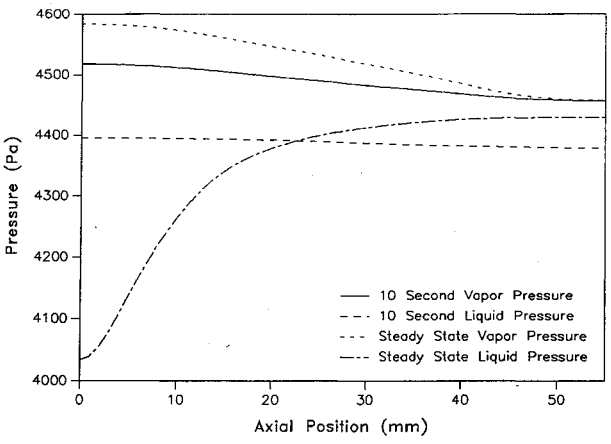

Fig. 11 Liquid and vapor pressure as a function of time and the axial position.

curvature to compensate for the total density changes resulting from the associated temperature change. Once the heat input reaches full load, the reverse liquid flow disappears, and the liquid mass flow rate gradually increases until it reaches a steady-state condition in which the liquid mass flow rate is equal to the vapor mass flow rate in any given section. This is more apparent in Fig. 11, which compares the pressure for a power level of 0.1 W and a wetting angle of 45 deg, as a function of axial position, for 10 s after startup and for steadystate. As illustrated, 10 s after startup the pressure of both the liquid and vapor are higher in the evaporator and gradually decrease with position, promoting flow away from the evaporator. At steady state, the liquid pressure is much lower in the evaporator and increases dramatically with position, promoting return flow back to the evaporator.

Finally, it is important to note that the pressure drops due to friction are much larger than for the pressure drop due to the vapor momentum change or the pressure drop due to the liquid momentum change.

Conclusions

A numerical model was developed and shown to accurately predict the steady-state transport limit of two previously tested micro heat pipes. The model was then used to evaluate the various parameters that govern micro heat pipe operation. The results of the modeling effort indicate that unlike traditional heat pipes, reverse liquid flow occurs in the liquid channels during startup and that the wetting angle is one of the most important factors contributing to the transport capacity and behavior of these types of heat pipes.

As mentioned, an earlier steady-state experimental investigation verified the operation of the trapezoidal micro heat pipe, and when compared with the analytical model, verified the trends predicted by the transient model at steady state. Although additional work is required to refine the model, this transient model can be used to accurately assess the effects of variations in the physical geometry, the amount or type of working fluid, and the power levels.

Although the transient numerical model has been shown to predict the steady-state performance limitations and operational characteristics with a reasonable degree of accuracy, no experimental data on the transient operational characteristics have been obtained. In addition, several factors that significantly affect both the steady state and transient behavior require continued study, including a determination of the effect of variations in the cross-sectional shape; the effect of variations in the amount of working fluid; and determination of just how small these devices can be and still continue to function.

Acknowledgment

Funding for this investigation was provided by the ITO Research and Development Corp., Osaka, Japan, the Texas Higher Education Coordinating Board, and the TAMU Center for Space Power.

References

[1]Peterson, G. P., and Ortega, A., "Thermal Control of Electronic Equipment and Devices," *Advances in Heat Transfer*, edited by J. Hartnett and T. Irvine, Academic, New York, 1990, pp. 181–314.

[2]Cotter, T. P., "Principles and Prospects of Micro Heat Pipes," *Proceedings of the 5th International Heat Pipe Conference*, JaTech, Tokyo, 1984, pp. 328–335.

[3]Peterson, G. P., Weichold M. H., and Mallik, A., U.S. Patent Pending, Patent Application # 380, 189, U.S. Patent and Trademark Office, filed on July 14, 1989.

[4]Babin, B. R., Peterson, G. P., and Wu, D., "Analysis and Testing of a Micro Heat Pipe During Steady-State Operation," American Society of Mechanical Engineers, New York, Paper 89-HT-17, Aug. 1989.

[5]Chi, S. W., *Heat Pipe Theory and Practice*, McGraw-Hill, New York, 1976.

[6]Dunn, P. D., and Reay, D. A., *Heat Pipes*, 3rd ed., Pergamon, New York, 1982.

[7]Collier, J. C., *Convective Boiling and Condensation*, McGraw-Hill, New York, 1981.

[8]Colwell, G. T., and Chang, W. S., "Measurements of the Transient Behavior of a Capillary Structure Under Heavy Thermal Loading," *International Journal of Heat and Mass Transfer*, Vol. 27, No. 4, 1984, 541–551.